Intelligence-Based Supervisory Control for Optimal Operation of a DCS-Controlled Grinding System

Ping Zhou, Tianyou Chai, *Fellow, IEEE*, and Jing Sun, *Fellow, IEEE*

***Abstract*—Optimizing the final grinding production indices (GPIs), which include the product particle size and the grinding production rate, to meet the overall manufacturing performance requirements is the main function of automatic control of a grinding circuit (GC). However, the complex and time-varying nature of the GC process dictates that these GPIs cannot be optimized solely by the lower-level distributed control systems (DCS), therefore an operator is often incorporated to manually determine the set-points for the DCS using his/her operational experience. With a human being involved, the performance and even the safety and stability of the GC operation is subject to human errors. Focusing on this practical challenge, this paper proposes an intelligence-based supervisory control strategy that consists of a control loop set-point optimization module, an artificial neural network-based soft-sensor module, a fuzzy logic-based dynamic adjustor, and an expert-based overload diagnosis and adjustment module to perform the control tasks for the GC system. This hybrid system can automatically adjust the set-points for the DCS-controlled grinding system in response to the changes in boundary conditions or the imminent overload conditions, thereby eliminating the need for an operator. Practical applications have shown the validity and effectiveness of the proposed approach.**

***Index Terms*—Fuzzy logic, grinding circuit (GC), optimization, process monitoring, soft-sensor, supervisory control.**

I. Introduction

MINERAL grinding circuit (GC) is widely used in industrial process to reduce the particle size of ore such that valuable mineral constituents can be decomposed and recovered in the subsequent beneficiation operation [1]–[4]. The grinding production indices (GPIs), namely the product particle size (PPS) and the grinding production rate (GPR), are the key metrics indicating the grinding product quality and process efficiency. In general, it is desirable to control the PPS within a specified range suitable for the subsequent beneficiation process while maximizing the GPR. Moreover, for safe operations the grinding mill load (GML) should be monitored closely to avoid overloading [4], [5].

Most industrial GCs in mineral processing are controlled by multi-loop proportional-integral (PI)/proportional-integral derivative (PID)-based distributed control systems (DCS). The lower-level DCSs are used to realize regulation and other control functions by various control loops such as single control loops, feed-forward control loops and cascade control loops. Each control loop consists of a complete set of control components such as sensors, actuators and controllers. If the PI/PID control algorithms employed are well developed, optimal tracking of the controlled variables with respect to their set-points can be achieved in lower-level control loops [6]–[13].

Given the multi-loop GC system, even when the performance of each control loop is satisfactory, the overall operation performance of the process may not meet the manufacturing requirements due to the interactive and complex nature of the GCs. In general, these GPIs are difficult to measure online and are closely related to the outputs of lower-level control loops. The associated dynamic characteristics between the GPIs and the key process variables controlled by the lower-level control loops are generally very intricate, involving complicated nonlinearities and strong cross couplings. Furthermore, accurate dynamic models are difficult to obtain because the dynamic behavior of the grinding operation is affected by many factors such as ore hardness, size distribution of the feed ores, grinding media, and the dimensions of metal spirals, etc. All these factors vary with time, and will be considered as boundary conditions of the grinding process operation.

To achieve a specified overall performance of the process operation, the higher-level supervision and control is always required to provide the appropriate set-points of DCS controllers according to the operating environment and boundary conditions [7]–[13]. In practice, the supervision control is handled by experienced operators. Through observing the status of the process operation, the operators will adjust the set-points for the control loops to keep the GPIs within reasonable ranges. Since the ore's hardness, size distribution and some other boundary conditions change frequently, the manual operation cannot always accurately define the set-points in time. Consequently, the GPIs may not be controlled within the required ranges, leading to possible mill overloading or other faulty working conditions.

Because an accurate mathematical model of the grinding process is difficult to obtain, most well-established control

Manuscript received June 15, 2011; accepted December 10, 2011. Manuscript received in final form January 03, 2012. Date of publication January 31, 2012; date of current version December 14, 2012. Recommended by Associate Editor D. Liu. This work was supported in part by the National Natural Science Foundation of China (61104084, 61020106003), in part by the Guangdong Education University-Industry Cooperation Projects (2010B090400410), in part by the FRFCU of China (N090608001), in part by the Creative Research Groups of China under Grant (60821063), in part by the GFG from the China PSF (2011M500567), in part by the 973 Program of China (2009CB320601), and in part by the 111 Project of China (B08015).

P. Zhou and T. Y. Chai are with the State Key Laboratory of Synthetical Automation for Process Industries, Northeastern University, Shenyang 110819, China (e-mail: zhouping@mail.neu.edu.cn).

J. Sun is with the Department of Naval Architecture and Marine Engineering and the Department of Electrical Engineering and Computer Science, University of Michigan, Ann Arbor, MI 48109 USA (e-mail: jingsun@umich.edu).

Color versions of one or more of the figures in this paper are available online at http://ieeexplore.ieee.org.

Digital Object Identifier 10.1109/TCST.2012.2182996

methodologies (e.g., model predictive control, self-optimization control, real-time optimization control, and direct online linear optimal control, etc. [13]–[16]) are not applicable. On the other hand, intelligent control methods (such as fuzzy logic, ANN, case-based reasoning and expert system, etc. [1], [3], [4], [7]–[12], [17]) have been applied to control many complex industrial processes due to their flexible requirements on the process model and their capability to incorporate human experience. Therefore, these intelligent methods are deemed to be more suitable to establish the process model and to develop the control system for the grinding process.

This paper presents an intelligence-based hybrid approach for a supervisory control system for the complex GC. This hybrid system can replace the human operator by auto-adjusting the proper set-points for the grinding system as the boundary condition varies. The system consists of a loop set-point optimization module (LSOM), an ANN-based PPS soft-sensor module (PSM), and a fuzzy dynamic adjustor (FDA). The LSOM is used to provide optimal nominal set-points for the loop controllers. The PSM is employed to generate the estimated value of PPS online and the FDA is utilized to compensate the effects of variations in the boundary condition. With the help of an expert-based overload diagnosis and adjustment module (ODAM), a strategy is incorporated to detect and mitigate of imminent mill overload conditions to ensure safe process operation. The successful demonstration of the proposed intelligent supervisory system in a practical application has confirmed the effectiveness of the proposed control system.

II. Grinding Circuit System Description

A. Process Description

The mineral grinding circuit studied here operates in a closed-loop mode as shown in Fig. 1. The system includes a grate ball mill, a spiral classifier and associated solids feeding conveyors. The principal specifications of the GC are shown in Table I and the key components involved include the following.

- The ball mill, which is a cylindrical shell that rotates around its axis at a fixed speed driven by a motor, with heavy metal balls called grinding media inside the cylinder. Due to the knocking and tumbling actions of the grinding media within the revolving mill, ores are crushed to fine particles.
- The spiral classifier. It is a classification unit and is used to filter powders grinded from the mill and to transfer the coarse materials to the feeding part of the mill and discharge the filtered fine materials through the overflow pipe. It works according to the principle that different granules (with various sizes and weight) sink at different speeds in liquids.

The variables in Fig. 1 are explained as follows.

d_{r}	Density of the classifier recycle (%).
o_{r}	Ore mass in the classifier recycle (t/h).
o_{f}	Fresh ore feed rate (t/h).

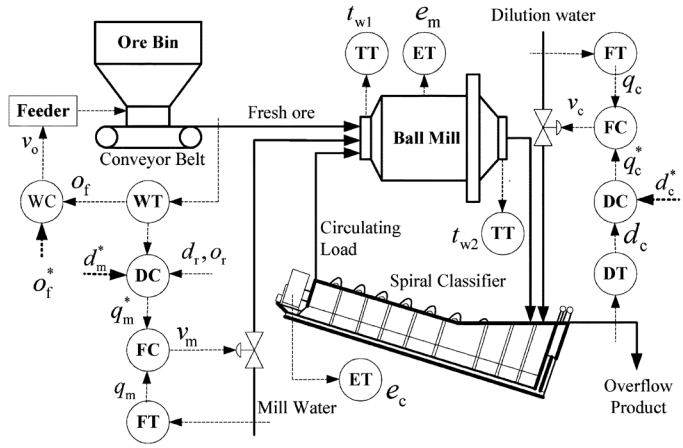

Fig. 1. Schematic diagram of mineral grinding circuit system.

TABLE I
Principal Specifications of the Grinding Circuit

Equipment	Specification
Grate ball mill	ϕ 3200mm×3500mm; Slurry volume: 25.3m^3; Rotate speed: 18.5r/min; Maximal medium load:54t
Spiral classifier	High weir 2FLG-ϕ 2400mm; Spiral rotate speed: 3.5r/min; Decline angle: 17°; Throughput: 80t/h.

d_{m}	Pulp density in the mill (%).
d_{c}	Flurry density of the classifier overflow (%).
$q_{\mathrm{m}}, q_{\mathrm{c}}$	Feed rate $(\mathrm{m}^3/\mathrm{h})$ of the mill water and the dilution water, respectively.
$v_{\mathrm{m}}, v_{\mathrm{c}}$	Valve position (%) of q_{m} and q_{c}, respectively.
$e_{\mathrm{m}}, e_{\mathrm{c}}$	Current (A) through the ball mill and the classifier, respectively.
$t_{\mathrm{w1}}, t_{\mathrm{w2}}$	Temperature $(^\circ\mathrm{C})$ of the ball mill's front-axis and rear-axis, respectively.
-C, -T	Controller and instrument, respectively.
W-, F-, D-, E-, T-	Respectively express weighing, flow rate, density, current, and temperature.
superscript $*$	Setpoint of the relevant control loop.

When the grinding process operation starts, the fresh coarse ore from an ore bin is fed onto a conveyer belt by a vibratory feeder at a certain speed, and then conveyed continuously into the ball mill together with a certain amount of mill water. A continuous flow of the mixed ore slurry is discharged from the mill. The slurry is diluted by the dilution water, and then flows into the lower end of the spiral classifier for classification. The coarser particles are enriched at the bottom, transported to the upper end of the spiral classifier and then recycled back to the mill for regrinding. As the product of this grinding procedure, the fine particles in the slurry overflow across a weir and are then transported to the subsequent processing facility.

B. Control Problem and Process Dynamic Characteristics

For the GC, there are two important GPIs, namely the PPS and the GPR, which define the process quality and efficiency but cannot be measured online continuously.

- The PPS, which is usually defined as the fraction of particles in spiral classifier overflow passing a sieve of -200 mesh aperture (% $<$200 mesh), is the most important quality index that directly affects the performance of the subsequent beneficiation process in terms of the product concentration grade and the metal recovery rate.
- The GPR, which is generally expressed by the mill throughput and the mill operative ratio (the percent of mill available time to production calendar time), is another important index that directly relates to the production performance of the mineral processing process.

For a given beneficiation process, there exists an optimal range of PPS within which the best beneficiation can be achieved. Oversizing and undersizing are disadvantageous for the beneficiation of the valuable minerals and have a negative economic impact. Therefore, the PPS should be controlled within its desired range $(s_{\rm d} - s_\Delta, s_{\rm d} + s_\Delta)$, where $s_{\rm d}$ is the set-point or desired value of the PPS, and s_Δ is the allowed fluctuation coefficient. Once the PPS is controlled within the desired range, the GPR should be maximized. Moreover, the GML needs to be monitored closely for the following reasons.

- First, the GML is an important factor that affects the PPS and GPR closely.
- Second, when the GML is too large, it will cause mill blockage and grinding interruption if it is not detected and mitigated in time.

The grinding system studied here has some inherent characteristics that have significant control implications, including the following.

- *Time delays*: Since the mill, the spiral classifier, and the conveying devices are all typical time-delay equipments, large lag-times exist in the GC. Indeed, it is a long period from the time when the fresh ore is fed into the mill to the time when the PPS index is measured in the overflow slurry of classifier.
- *Couplings between indices*: The interactions between the PPS and the GPR, and the associated dynamic characteristics between these indices and the key process variables are complicated and generally difficult to be coordinated. For example, an increase in the fresh ore feed rate $o_{\rm f}$ (t/h) may allow an increase in mill throughput, thus improve the GPR, but could result in a coarser PPS. Conversely, a decrease in $o_{\rm f}$ produces a finer PPS, however, may result in a lower GPR.
- *Uncertainties and disturbances*: The main external disturbances, such as the fluctuation in ore hardness $k_{\rm m}$ and size distribution $k_{\rm r}$ of the feed ores, may change abruptly with time, causing large perturbations in the control loop. Moreover, the internal disturbances, caused by coupling effects and time-varying parameters (e.g., grinding media and dimensions of metal spirals, etc.), may affect the dynamic features and even result in unstable operation of GC.
- *Lack of measurement for critical parameters*: The GPIs (i.e., PPS, GPR), the GML, and some other key process parameters, such as the circulating load $c_{\rm r}$ (t/h), and the pulp density in the mill $d_{\rm m}$ (%), cannot be measured online, and large time delays exist in their offline assaying, in addition to the process inherent time delays. This may lead to sluggish system response, thereby representing a serious obstacle in achieving good process operation.

C. DCS-Controlled Grinding System With Human Supervision

Due to the above mentioned process intricate characteristics, accurate dynamical models are difficult to obtain. Thus, it is ineffective to use existing model-based control methods developed for chemical plants to perform the required control design for the grinding process. In fact, even when knowledge-driven control methods are used for the grinding process in a few countries, such as in South Africa [1], the multiple PI/PID-based lower-level DCS strategies have always been used with human supervisions. The DCSs are then designed to force the key process variables to track given set-points while assuring closed-loop stability. For the GC under study, the control loops incorporated include the following.

- A single control loop used to maintain $o_{\rm f}$ around $o_{\rm f}^*$ by regulating the frequency of the feeder motor $v_{\rm o}$ (Hz).
- A feed-forward control that keeps $d_{\rm m}$ around a desired value $d_{\rm m}^*$ by setting the mill water feed rate $q_{\rm m}({\rm m}^3/{\rm h})$. The valve position $v_{\rm m}$ (%) of mill water is manipulated to regulate the control loop of $q_{\rm m}$.
- A cascade control loop used to control the flurry density of the classifier overflow $d_{\rm c}$ (%) around its set-point $d_{\rm c}^*$, and the valve position of dilution water $v_{\rm c}$ (%) is manipulated to regulate the dilution water feed rate $q_{\rm c}({\rm m}^3/{\rm h})$.

As shown in Fig. 1, the configuration of the DCSs is made up of the following major instruments and actuators.

- A nuclear apparatus WT is located on the conveyor belt to measure $o_{\rm f}$ online.
- Two electromagnetic flowmeters FT are mounted on the pipelines of the mill water and the dilution water to measure $q_{\rm m}$ and $q_{\rm c}$, respectively.
- A radioisotope densimeter DT is mounted on the pipeline of the classifier overflow and used to measure $d_{\rm c}$ online.
- Two galvanometers ET are connected to the drive motor to measure the current through the mill motor (mill current for short) $e_{\rm m}$ (A) and the current through the classifier motor (classifier current for short) $e_{\rm c}$ (A), respectively.
- Two platinum resistance transducers TT are connected to the ball mill's front- and rear- axis to detect their running temperatures $t_{\rm w1}, t_{\rm w2}$, respectively.
- Two electric valves are used to regulate $q_{\rm m}$ and $q_{\rm c}$.
- A transducer is used to regulate $o_{\rm f}$.

For the lower-level DCSs, PI/PID control strategies are often applied. Because $d_{\rm m}$ cannot be measured, a model-based feed-forward controller as shown in (1) is used to compute the desired mill water feeding rate $q_{\rm m}^*$ according to the given $d_{\rm m}^*$

$$q_{\rm m}^* = \left[(100o_{\rm f} + o_{\rm r})/\left(o_{\rm f}d_{\rm m}^*\right) - o_{\rm r}/(o_{\rm f}d_{\rm r}) - 1\right] o_{\rm f} \qquad (1)$$

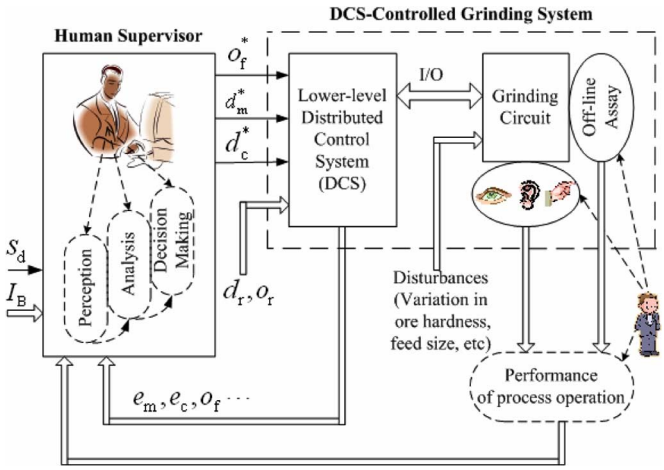

Fig. 2. DCS-controlled grinding system with human supervision. I_{B}: boundary conditions which mainly include k_{m}, k_{r}, and bounds of some process variables; $k_{\mathrm{m}}, k_{\mathrm{r}}$: ore hardness and size distribution of the feed ores, respectively; s_{d}: desired value of the PPS (% <200 mesh).

TABLE II
OPERATING PHASES OF MANUAL SUPERVISION

Phase	Operation
Perception	To obtain the process data from the grinding system using instruments together with visual or audio inspection on the operating status of GC.
Analysis	By means of the knowledge-based model of the process in his/her brain, to estimate the immeasurable controlled variables and disturbance variables.
	To establish the relationships between the loop set-points and the performance of process operation, and the internal relationships between the set-points of the loop controllers, according to human experience.
Decision-making	To determine the proper set-points for the DCS.

where d_{r} denotes density of classifier recycle (%), o_{r} is the ore mass in classifier recycle (t/h).

To maintain satisfactory overall performance, engineers are always required, as shown in Fig. 2, to determine the proper set-points for the DCS controllers according to their perceived operating conditions and boundary conditions. Such manual supervision can be summarized as shown in Table II.

Due to the large process disturbances, uncertain process dynamics, and coupling effects, the grinding operating conditions often vary with time. Moreover, lack of adequate operational experiences also prevents the operator to be 100% effective. These factors make it difficult for the human driven operation shown in Fig. 2 to achieve the proper set-points in a timely fashion, which in turn may lead to the GPIs exceeding the desired range, or even mill overloading and other faulty conditions. Therefore, the human-supervised DCSs have the safety, stability, and reliability concerns.

III. INTELLIGENCE-BASED SUPERVISORY CONTROL STRATEGY

From the above analysis, the key issue of optimizing the operation of the DCS-controlled grinding system is how to adjust online the set-points of the control loops under either the variation of the operating points or in the presence of potential overloading conditions, so that the target GPIs can be achieved with certainty and overload conditions can be eliminated. To address such a challenging issue, an intelligence-based supervisory control scheme is proposed by combining the steady-state optimization [18] and hybrid intelligent techniques. A framework for the higher-level supervision control system is established for the DCS-controlled grinding system as shown in Fig. 3. This system consists of a loop set-point optimization module (LSOM), an ANN-based PPS soft-sensor module (PSM), a fuzzy dynamic adjustor (FDA), and an expert-based overload diagnosis and adjustment module (ODAM). This supervisory control system is intended to replace the human operator by auto-adjusting the set-points for the DCS in response to the changes in boundary conditions or the looming overload conditions. The major components of the proposed system are described as follows.

- The online LSOM, using quadratic programming optimization technique [18], provides the optimal nominal set-points Y_0^* for the lower-level DCS controllers.
- The PSM overcomes the difficulty of measuring PPS in real-time. It offers a solution to estimate PPS on time using an ANN-based soft-sensor technique.
- The FDA, consisting of a main adjustor and an auxiliary adjustor, is used to compensate the effects of the variation in the grinding operating conditions.
  - The main adjustor responds to the error $\Delta s_{\mathrm{pd}} = s_{\mathrm{p}} - s_{\mathrm{d}}$ so as to yield the compensating increments ΔY_{M}^* for the loop set-points.
  - The auxiliary adjustor generates the adjustment increments ΔY_{A}^* for the loop set-points according to the error $\Delta s_{\mathrm{ad}} = s_{\mathrm{a}} - s_{\mathrm{d}}$.
- The ODAM is composed of a statistical process control (SPC) unit, an overload diagnosis model and an overload adjustor.
  - The SPC is used to identify and track the variation of the mill current.
  - The overload diagnosis model is applied to detect the potential mill overload condition with an expert system technique.
  - The overload adjustor can auto-adjust the grinding system with ΔY_{L}^* to move the GML away from the faulty overloading condition.

The five operation phases of the intelligent supervision system are summarized in Table III. When the grinding system is running, the LSOM will find the optimal set-points Y_0^* under various production constraints I_{B}. Once Y_0^* is determined, the LSOM will be switched off, and the grinding system will work at this initial set-points by driving the DCS outputs towards their set-points. Meanwhile, the PSM, the FDA, and the ODAM will be switched on. If the estimated PPS s_{p} is outside the desired range $(s_{\mathrm{d}} - s_{\Delta}, s_{\mathrm{d}} + s_{\Delta})$, the main adjustor will response to the error Δs_{pd} to yield ΔY_{M}^* for the loop set-points by using an algorithm that can enhance the GPR effectively. Moreover, the sampled PPS $\mathrm{s_a}$ will be provided periodically by off-line assays, so that the auxiliary adjustor can carry out the needed adjustment whenever $\mathrm{s_p}$ is outside the range $(\mathrm{s_d} - \mathrm{s_\Delta}, \mathrm{s_d} + \mathrm{s_\Delta})$ for certain amount of time.

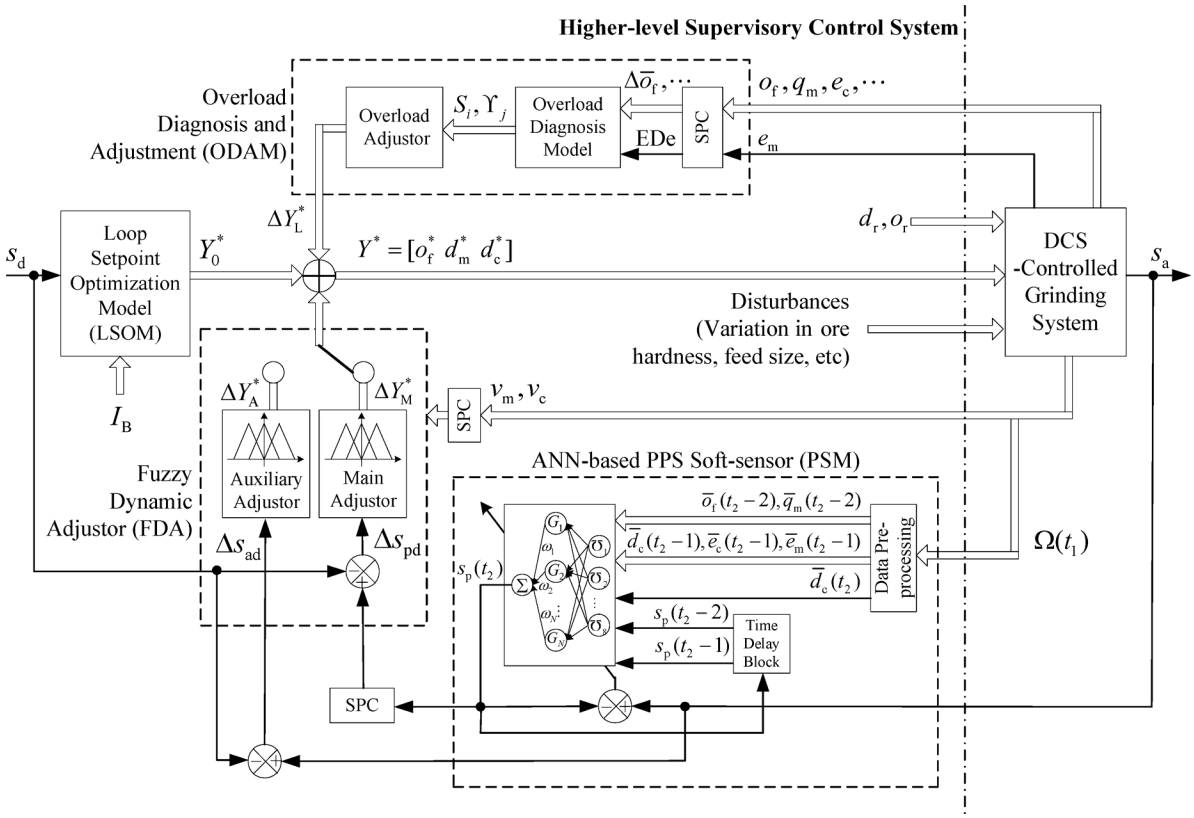

Fig. 3. Strategy diagram of intelligence-based supervisory control.

TABLE III
OPERATING PHASES OF INTELLIGENT SUPERVISION

Operating phases of supervision	LSOM	PSM	FDA		ODAM
			Main adjustor	Auxiliary adjustor	
Search the optimal nominal set-points	on	off	off	off	off
Estimation of the PPS online	off	on	on	on	on
Main adjustment on the running grinding system under the normal working condition	off	on	on	on	on
Auxiliary adjustment on the running grinding system under the normal working condition	off	on	on	on	on
Adjustment on the running grinding system under the fault working condition	off	on	off	off	on

The variables in Fig. 3 are explained as follows.

$s_{\mathrm{a}}, s_{\mathrm{p}}$	Sampled and estimated value of the PPS (% <200 mesh), respectively.
$\Delta s_{\mathrm{pd}}, \Delta s_{\mathrm{ad}}$	Error between s_{p} and s_{d}, and between s_{a} and s_{d}, respectively.
$Y_0^* = [o_{\mathrm{f},0}^* d_{\mathrm{m},0}^* d_{\mathrm{c},0}^*]$	Nominal set-points of loop controller.
$\Delta Y_{\mathrm{M}}^*, \Delta Y_{\mathrm{A}}^*, \Delta Y_{\mathrm{L}}^*$	Adjusted increments of Y^*, subscript "M", "A", "L" denotes the main, the auxiliary, and the overload adjusting, respectively.
$\Omega, \mho$	Secondary variable set and input vector of the PSM, respectively.
S_i, Υ_j	Overload conditions and their reliabilities, respectively.

Moreover, if an imminent overload condition is detected by the overload diagnosis model, the FDA will be switched off, and the overload adjustor will adjust the grinding system rapidly. As long as the DCS outputs track their updated set-points, the operating grinding system will eliminate the overload conditions and achieve the desired overall performance.

Remark 1: In the proposed hybrid control methodology, although each control element is well known, their innovative combination can generate better and more reliable performance because of the following features.

- While the nominal performance is maintained by the LSOM, improved performance can always be achieved by the FDA. The safety of the whole process operation can be ensured by the ODAM. The key problem of PPS not being measured continuously with conventional methods is solved by the PSM.
- The combination of the LSOM, PSM, FDA, ODAM, and the lower-level DCS poses a novel optimization and closed-loop control framework for the PPS from the lower level to the higher level, which is usually beyond the

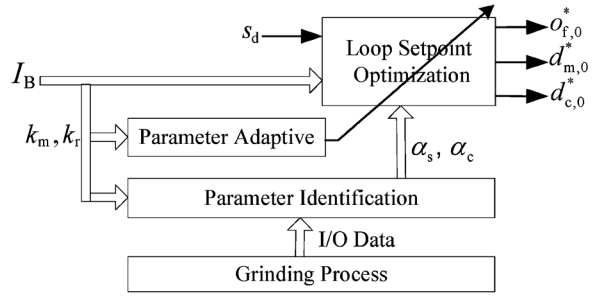

Fig. 4. Strategy diagram of the LSOM.

capability of the conventional control methods. Moreover, the synergistic integration of the modules helps to improve GPR while assuring the safety of the whole process operation.

Remark 2: In contrast to the conventional setpoint tracking control, the range optimized control scheme proposed herein for the PPS index control is much more suited for the control of production indices. The range optimized control can maintain system stability as it does not require frequent adjustment to the controlled system. This means that it can reduce unnecessary adjustments in response to allowable errors in the measurement of production indices and other process variables.

Remark 3: Since some process parameters used in our control strategy are based on their statistical values, the transitory values of such relevant variables are pre-processed statistically by using the SPC technique to make them useful for the corresponding control modules. The SPC technique was pioneered by Shewhart in the early 1920s [18], [19], it uses statistical methods to understand, analyze, interpret numerical information. The SPC is also used in our control strategy to identify and track variation of the mill current for the ODAM.

IV. Intelligent Supervisory Control Algorithm

A. Loop Set-Point Optimization Algorithm

The LSOM, as shown in Fig. 4, is employed to calculate the steady-state optimal set-points

$$Y_0^* = \arg \min_{Y=[o_f d_m o_c]} J(Y)$$

for each control loop by minimizing

$$\begin{aligned} &J(Y) = \|\mathrm{PPS} - s_d\|^2 \\ &\text{s.t.} \quad \text{a)} \begin{bmatrix} \mathrm{PPS} \\ c_r \end{bmatrix} = \begin{bmatrix} f_s(k_m, k_r, \alpha_s) \\ f_c(k_m, k_r, \alpha_c) \end{bmatrix} Y^T \\ &\qquad \text{b)} \begin{bmatrix} s_d - s_\Delta \\ c_{r,\min} \\ Y^T_{\min} \end{bmatrix} \le \begin{bmatrix} \mathrm{PPS} \\ c_r \\ Y^T \end{bmatrix} \le \begin{bmatrix} s_d + s_\Delta \\ c_{r,\max} \\ Y^T_{\max} \end{bmatrix} \end{aligned} \quad (2)$$

where the constraint a) denotes the steady-state model of PPS and c_r, and the constraint b) denotes the minimum and maximum limits of PPS, c_r, and Y; $f_s(\cdot), f_c(\cdot)$ are the coefficient function. For a given type of ore, the coefficients $\alpha_s = \{\alpha_{s,i}\}$, $\alpha_c = \{\alpha_{c,i}\}$ in $f_s(\cdot), f_c(\cdot)$ are determined and updated using identification strategies based on process excitation.

TABLE IV
Numerical Demarcation of K_M and K_R

Numerical value		1	1.5	2	2.5	3
Linguistic description	k_m	bad	relatively bad	medium	relatively good	good
	k_r,	big	relatively big	medium	relatively little	little

Remark 4: A practical mineral processing plant usually handles several types of ore, such as pyrite, siderite, hematite, limonite, and their mixture. The physical property of ore grindability will change if the ore type is changed, leading to a change in the optimization model. Note that k_m (hardness) and k_r (size distribution) can reflect the ore grindability capacity well, we can use them as two adaptive factors to adjust the parameters of process model according to the ore type. Given the difficulty in numerically expressing k_m and k_r, five ordered numerical values are utilized to demarcate the linguistic description of k_m and k_r in practice, as shown in Table IV. In practice, the values of k_m and k_r are usually demarcated by domain experts or experienced operators according to the type or the components of processed ore.

Since the optimization problem considered here contains a quadratic objective function with linear constraints, the optimal solution can be easily found using the popular QP algorithm.

B. ANN-Based PPS Soft-Sensor Algorithm

Given that the PPS cannot be measured continuously, the soft-sensor technique is employed to estimate the PPS online. Among the existing PPS soft-sensor approaches, the ANN-based method and the ARMAX model-based method [20]–[22] have been applied widely. The ARMAX model usually has narrow range of applicability for nonlinear processes. To deal with the nonlinear problem associated with PPS and to improve estimation performance, we resort to the RBF-ANN technique for the modeling task since the RBF-ANN offers the distinctive ability to learn complex nonlinear relationship without requiring knowledge of the model structure [20].

The developed PSM has three-layer RBF-ANN structures, and realizes the nonlinear mappings in (3)

$$\begin{aligned} s_p(t_2) &= \sum_{i=1}^{N} \omega_i G_i\left(\|\mho - C_i\|\right) \\ G_i\left(\|\mho - C_i\|\right) &= \exp\left(-\|\mho - C_i\|^2 / 2\sigma_i^2\right),\ i = 1, \ldots, N \end{aligned} \quad (3)$$

where $\mho = [\overline{d}_c(t_2)\overline{d}_c(t_2-1)\overline{e}_m(t_2-1)\overline{e}_c(t_2-1)\ \overline{o}_f(t_2-2)\overline{q}_m(t_2-2)s_p(t_2-1)s_p(t_2-2)]^T$ is the network input vector, $\Omega = \{o_f, q_m, d_c, e_m, e_c\}$ are the selected secondary variables according to physical analysis (o_f, q_m, and d_c are the manipulated variables that affect the PPS mostly. e_m and e_c are the state variables that relate to the PPS closely), $G_i(\cdot)$ is the hidden Gaussian radial function, C_i and σ_i are the centres and radiuses of $G_i(\cdot)$, respectively, ω_i are the linear connection weights of the output layer, N is the number of hidden neurons.

In (3), $\overline{d}_c(t_2)$ is determined as

$$\overline{d}_c(t_2) = t_1 \sum_{k=1}^{t_2/t_1} \overline{d}_c(kt_1) \Big/ t_2$$

TABLE V
NETWORK TRAINING PROCEDURE

Step 1:	Let k=0, N=8, and input the training samples into the network.
Step 2:	Set the basis functions number as N=N+k
Step 3:	Employ the k-means clustering algorithm to obtain C_i, i=1,…,N.
Step 4:	Assign $\sigma_i = D/\sqrt{2N}$, where D is the maximum distance of these selected centres.
Step 5:	Apply the weighted RLS algorithm to learn ω_i.
Step 6:	Evaluate the estimation performance of the trained RBF-ANN: If the estimations can meet the specified accuracy, then goto Step 7. Else let k=k +1, and goto Step 2.
Step 7:	Stop training.

where t_1 denotes the sample time constant of the DCS (in seconds), t_2 denotes the soft-sensor time constant. To eliminate higher frequency noise fluctuations, t_2 is determined as $t_2 = 30t_1$. Moreover, to capture the system dynamics, the time series and time delays of the input and output variables have been taken into account in (3).

The Gaussian radial function parameters C_i and σ_i, and the connection weights ω_i are important to the nonlinear mapping ability of the RBF-ANN. Many algorithms are available to train the RBF-ANN. In this paper, the unsupervised k-means clustering algorithm [8] is used to determine C_i, and the weighted RLS algorithm [8], [23] is employed to learn ω_i. The procedure used for RBF-ANN training is listed in Table V. The description of the detailed k-means algorithm and the weighted RLS algorithm are omitted here, as they are standard and can be found in existing literatures, such as in [8] and [23].

Remark 5: In developing the RBF-ANN based soft-sensor, we used available data without doing additional industrial experiments. This approach has the least intervention to process operation and safety. However, over long time operation, the system may drift due to time-varying nature of the grinding system, and the soft-sensor system may become less accurate. This problem can be coped with online adaptation of model parameters in the soft-sensor system. However, this will increase the system burden and interfere with other system requirements. Therefore, periodical offline learning for the ANN-based soft-sensor system is adopted in this paper. If the trained ANN-based soft-sensor system running for a long time or the process operation changes significantly, the RBF-ANN sensor has to be retrained in order to give a valid estimation.

C. Multivariable Fuzzy Dynamic Adjust Algorithm

The boundary conditions of the grinding system often vary with time, resulting in the operating points drifting away from its initial optimal points. To mitigate the effects of these variations, an adjustment mechanism is required to modify the loop setpoints on time.

Since the grinding process is a multivariable system with extremely complex properties, conventional methods which require an accurate mathematical model are not suitable for this higher-level adjustment. On the other hand, experience and knowledge of the human operator provide a good qualitative model for the adjustment system, which can be more easily imitated by the fuzzy logic system.

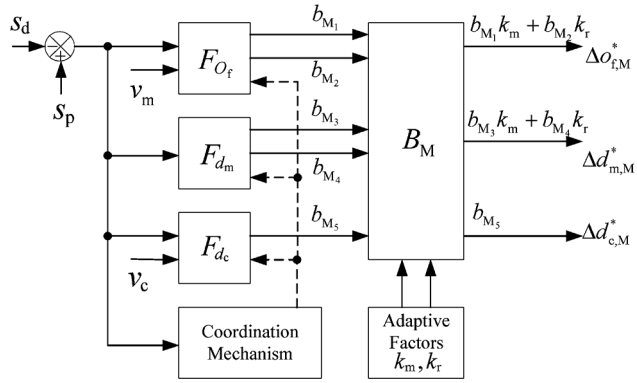

Fig. 5. Structure of fuzzy-based main adjustor.

The fuzzy dynamic adjustor (FDA) developed in this paper consists of a main adjustor and an auxiliary adjustor, which realize the following multivariable nonlinear mappings, respectively:

$$\begin{cases} \underbrace{\left(\Delta o^*_{\mathrm{f,M}}, \Delta d^*_{\mathrm{m,M}}, \Delta d^*_{\mathrm{c,M}}\right)}_{\Delta Y^*_{\mathrm{M}}} = \phi_{\mathrm{M}}(\Delta s_{\mathrm{pd}}, v_{\mathrm{m}}, v_{\mathrm{c}}) \\ \underbrace{\left(\Delta o^*_{\mathrm{f,A}}, \Delta d^*_{\mathrm{m,A}}, \Delta d^*_{\mathrm{c,A}}\right)}_{\Delta Y^*_{\mathrm{A}}} = \phi_{\mathrm{A}}(\Delta s_{\mathrm{ad}}, v_{\mathrm{m}}, v_{\mathrm{c}}) \end{cases} \tag{4}$$

where

$$\begin{cases} \Delta s_{\mathrm{pd}} = s_{\mathrm{p}} - s_{\mathrm{d}} = \sum_{i=1}^{k_1} [i s_{\mathrm{p}}(it_2)] \Big/ \sum_{i=1}^{k_1} i - s_{\mathrm{d}}, k_1 \in Z^+, k_1 > 1 \\ \Delta s_{\mathrm{ad}} = s_{\mathrm{a}} - s_{\mathrm{d}} \end{cases} \tag{5}$$

v_{m} and v_{c} are regarded as the relative influence factors. In (5), to simulate the moving average features of the human perception of input signals, the transitory output $s_{\mathrm{p}}(t_1)$ of the soft-sensor model is processed statistically by the SPC before being used by the FDA.

Because the detailed realization arithmetic of the auxiliary adjustor is similar to the main adjustor, we only discuss the fuzzy dynamic adjustment algorithm for the main adjustor. The module structure of the main adjustor is shown in Fig. 5, which consists of a coordination mechanism and three fuzzy inference mechanisms (i.e., $F_{o_{\mathrm{f}}}, F_{d_{\mathrm{m}}}, F_{d_{\mathrm{c}}}$).

The coordination mechanism is employed to provide an adjustment scheme that can enhance the GPR with a desired product quality. The detailed coordinating flowsheet is shown in Fig. 6, where $\uparrow, \downarrow$ and $\leftrightarrow$ stand for positive adjustment, negative adjustment, and no adjustment, respectively. The fundamental idea behind can be described as follows.

- If the PPS is too fine, one should first increase o^*_{f} while keeping $d^*_{\mathrm{m}}, d^*_{\mathrm{c}}$ unchanged to enhance the mill throughput.
- If the PPS is too coarse, in order to keep the mill throughput, one should adjust $d^*_{\mathrm{m}}, d^*_{\mathrm{c}}$, whereas keeping the value of o^*_{f}.

Fig. 7 shows the composition of each fuzzy inference mechanism, which uses the membership functions as shown in Fig. 8. Considering that the adjusted increments ΔY^*_{M} are sensitive to

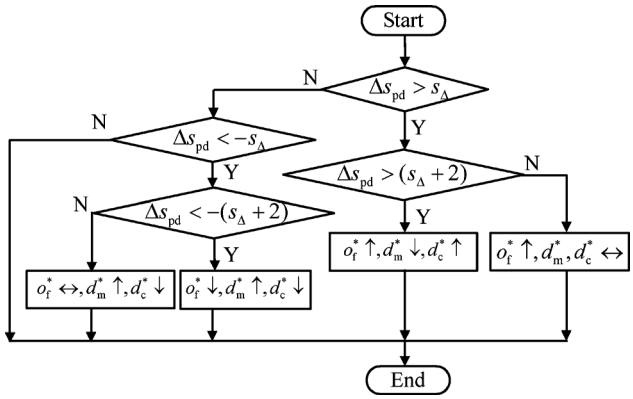

Fig. 6. Coordinating flowsheet of the coordination mechanism.

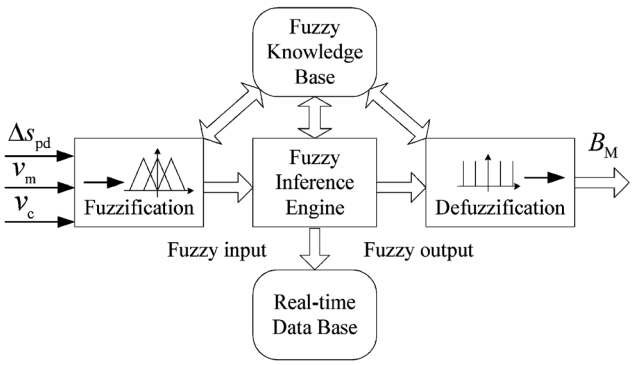

Fig. 7. Composition of the fuzzy inference mechanism.

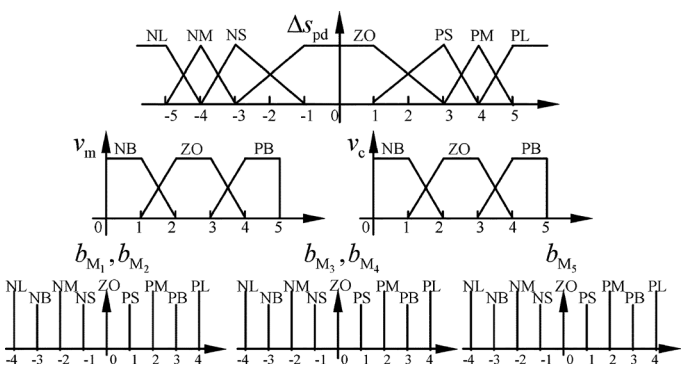

Fig. 8. Membership functions of $\Delta s_{\rm pd}$, $v_{\rm m}$, $v_{\rm c}$ and $b_{\rm M_1} \sim b_{\rm M_5}$.

ore properties, we incorporate two adaptive factors $k_{\rm m}$ and $k_{\rm r}$ for their expressions, i.e.,

$$\begin{bmatrix} \Delta o^*_{\rm f,M} \\ \Delta d^*_{\rm m,M} \\ \Delta d^*_{\rm c,M} \end{bmatrix} = \underbrace{\begin{bmatrix} b_{\rm M_1} & b_{\rm M_2} & 0 \\ b_{\rm M_3} & b_{\rm M_4} & 0 \\ 0 & 0 & b_{\rm M_5} \end{bmatrix}}_{B_{\rm M}} \begin{bmatrix} k_{\rm m} \\ k_{\rm r} \\ 1 \end{bmatrix}.$$

In Fig. 8, the universe of $\Delta s_{\rm pd}$ takes its true value. According to the practical requirements, the universes of $b_{\rm M_1} \sim b_{\rm M_5}$, $v_{\rm m}$, $v_{\rm c}$ are determined as listed in Table VI, respectively. The rule bases for each inference engine $F_{o_{\rm f}}$, $F_{d_{\rm m}}$, $F_{d_{\rm c}}$, extracted from the fundamental mechanism of process and knowledge of operators, are shown in Table VII, where codes

TABLE VI
UNIVERSES OF $\Delta Y^*_{\rm M}$, $v_{\rm m}$, $v_{\rm c}$

Parameters		$\Delta Y^*_{\rm M}$					$v_{\rm m}$,%	$v_{\rm c}$,%
		$\Delta o^*_{\rm f,M}$, t/h		$\Delta d^*_{\rm m,M}$,%		$\Delta d^*_{\rm c,M}$,%		
		$b_{\rm M_1}$	$b_{\rm M_2}$	$b_{\rm M_3}$	$b_{\rm M_3}$	$b_{\rm M_5}$		
Universes	-4	-1.6	-1.2	—	—	-3.5	—	—
	-3	-1.2	-0.8	-0.3	-0.15	-2.5	—	—
	-2	-0.8	-0.6	-0.2	-0.1	-1.5	—	—
	-1	-0.4	-0.2	-0.1	-0.05	-0.5	—	—
	0	0	0	0	0	0	0	0
	1	0.4	0.2	0.1	0.05	0.5	15	15
	2	0.8	0.6	0.2	0.1	1.5	30	30
	3	1.2	0.8	0.3	0.15	2.5	70	70
	4	1.6	1.2	—	—	3.5	85	85
	5	—	—	—	—	—	100	100

TABLE VII
FUZZY ADJUSTMENT RULE BASES FOR $F_{o_{\rm f}}$, $F_{d_{\rm m}}$, $F_{d_{\rm c}}$

$b_{\rm M_1}, b_{\rm M_2}/b_{\rm M_3}, b_{\rm M_4}/b_{\rm M_5}$		$v_{\rm m}$ or $v_{\rm c}$		
		NB	ZO	PB
$\Delta s_{\rm pd}$	NB	NB/PB/NL	NL/PB/NL	NL/PB/NB
	NM	NM/PM/NB	NB/PM/NB	NB/PM/NM
	NS	NS/PS/NM	NM/PS/NM	NM/PS/NS
	ZO	ZO/ZO/ZO		
	PS	PM/NS/PS	PM/NS/PM	PS/NS/PM
	PM	PM/NS/PS	PB/NM/PB	PM/NM/PB
	PB	PL/NB/PB	PL/NB/PL	PB/NB/PL

NL, NB, NM, NS, etc., are commonly used abbreviations for fuzzy sets. These fuzzy rules $\rm R_j$ could be expressed as the following fuzzy IF-THEN rule:

$$\mathrm{R}_j: \begin{cases} \text{IF } \Delta s_{\rm pd} \text{ IS } \Gamma_j(\Delta s_{\rm pd}) \\ \quad \text{AND } [v_{\rm m} \text{ IS } \Gamma_j(v_{\rm m}) \\ \quad\quad \text{OR } v_{\rm c} \text{ IS } \Gamma_j(v_{\rm c})] \\ \text{THEN} \begin{cases} (b_{\rm M_1} \text{ AND } b_{\rm M_2}) \text{ ARE } \Gamma_j(b_{\rm M_1}) \\ (b_{\rm M_3} \text{ AND } b_{\rm M_4}) \text{ ARE } \Gamma_j(b_{\rm M_3}) \\ b_{\rm M_5} \text{ IS } \Gamma_j(b_{\rm M_5}) \end{cases} \end{cases}$$
$$\Gamma_j(\cdot) \in \{\mathrm{NL}, \mathrm{NB}, \mathrm{NM}, \mathrm{NS}, \mathrm{ZO}, \mathrm{PS}, \mathrm{PM}, \mathrm{PB}, \mathrm{PL}\}.$$

To obtain the clear solutions of $\Delta Y^*_{\rm M}$, the centre of gravity method is utilized to defuzzify. Thus $B_{\rm M}$ can be calculated according to (6)

$$B_{\rm M} = \begin{bmatrix} \frac{\sum[\Theta(R_j)\Gamma_j(b_{\rm M_1})]}{\sum\Theta(R_j)} & \frac{\sum[\Theta(R_j)\Gamma_j(b_{\rm M_2})]}{\sum\Theta(R_j)} & 0 \\ \frac{\sum[\Theta(R_j)\Gamma_j(b_{\rm M_3})]}{\sum\Theta(R_j)} & \frac{\sum[\Theta(R_j)\Gamma_j(b_{\rm M_4})]}{\sum\Theta(R_j)} & 0 \\ 0 & 0 & \frac{\sum[\Theta(R_j)\Gamma_j(b_{\rm M_5})]}{\sum\Theta(R_j)} \end{bmatrix} \quad (6)$$

where weights $\Theta(R_j)$ are the memberships of each rule and calculated by the product algorithm.

D. Expert-Based ODAM Algorithm

Mill overload is a common faulty condition that occurs in grinding process operation, which can lead to poor product quality and even the collapse of grinding production if it is not detected and controlled in time. Therefore, the GML should be closely monitored to assure reliability and operation integrity.

This paper establishes an expert-based ODAM to detect the imminent mill overload condition and then adjust the setpoints of DCS to make sure that the GML stays away from the overload condition during its operation.

1) SPC-Based Statistical Analysis of e_{m}: According to the operation experience, e_{m} decreases markedly when the GML is decreased in the underload area, especially when the mill is overloaded. Therefore we can use this correlation to identify overload conditions. However, the dynamic behavior of the grinding process is affected by many factors, which vary with time, thus e_{m} always fluctuates. Therefore, it needs to be preprocessed before it can be used for diagnosis purpose. Since the process data of a normal operation can be described in terms of statistically independent observations that fluctuate around a constant mean, the SPC technique is employed to carry out statistical analysis of e_{m}, which can be described as follows:

$$\begin{cases} \overline{e}_{\mathrm{m}}(t_2) = \frac{t_1}{t_2} \sum_{k=1}^{t_2/t_1} e_{\mathrm{m}}(kt_1) \\ u_{e_{\mathrm{m}}}(t_3) = \frac{t_2}{t_3} \sum_{k=1}^{t_3/t_2} \overline{e}_{\mathrm{m}}(kt_2) \\ \delta_{e_{\mathrm{m}}}(t_3) = \sqrt{\frac{t_2}{t_3 - t_2} \sum_{k=1}^{t_3/t_2} \left[\overline{e}_{\mathrm{m}}(kt_2) - u_{e_{\mathrm{m}}}(t_3)\right]^2} \end{cases} \tag{7}$$

where t_3 is the time constant in calculating $u_{e_{\mathrm{m}}}$ and $\delta_{e_{\mathrm{m}}}$, here we set $t_2 = 30t_1$ and $t_3 = 20t_2$.

Following the West Electric Rule in the SPC field [18], [24], this paper proposes the following rules to judge whether e_{m} descends or not: *If at least one of the following conditions is true, then e_{m} is descending*

$$\begin{cases} \text{a. } \overline{e}_{\mathrm{m}}(\tau) < \overline{e}_{\mathrm{m}}(\tau - 1) < \left[u_{e_{\mathrm{m}}}(t) - 3\delta_{e_{\mathrm{m}}}(t)\right], \\ \qquad 3\delta \text{ control limit} \\ \text{b. } \overline{e}_{\mathrm{m}}(\tau) < \overline{e}_{\mathrm{m}}(\tau - 1) < \overline{e}_{\mathrm{m}}(\tau - 2) \\ \qquad < \left[u_{e_{\mathrm{m}}}(t) - 2\delta_{e_{\mathrm{m}}}(t)\right], \\ \qquad 2\delta \text{ control limit} \\ \text{c. } \overline{e}_{\mathrm{m}}(\tau) < \overline{e}_{\mathrm{m}}(\tau - 1) < \overline{e}_{\mathrm{m}}(\tau - 2) \\ \qquad < \overline{e}_{\mathrm{m}}(\tau - 3) < \left[u_{e_{\mathrm{m}}}(t) - \delta_{e_{\mathrm{m}}}(t)\right], \\ \qquad 1\delta \text{ control limit} \end{cases}$$

where $\tau < t$. For simplicity, this event is abbreviated as EDe.

2) Expert-Based Overload Diagnosis and Adjustment: As analyzed above, mill overload or decreasing of GML in the underload area will manifest e_{m} descend during the mill running. Therefore, it is unreliable to monitor the GML only by this single information. According to the operation experience, the reasons for the mill overload can be classified into too large o_{f}, too high d_{m}, and too bad ore properties (such as too large hardness, too coarse size). Therefore, one should monitor and adjust the GML using these multiplex information. It is noted that disproportion of grinding medium can also cause overloading. However, it is not considered here because the problem can be overcome by a rational scheme for the grinding medium adding.

The rules for overload diagnosis, extracted from the fundamental mechanism of grinding process and the knowledge of on-site operators, are listed in Table VIII, where λ_i stand for some adjustable thresholds. The antecedent of each production rule includes one main antecedent and several auxiliary antecedents. The main antecedent is the event of EDe, and the auxiliary antecedents are the variation of other relative variables. The conclusions are the overload conditions that caused by too larger $o_{\mathrm{f}}(S_1)$, or too higher $d_{\mathrm{m}}(S_2)$, or too bad ore property (S_3), and the corresponding reliability Υ_1 (high reliability) or Υ_2 (normal reliability).

TABLE VIII
RULES FOR OVERLOAD DIAGNOSIS

Antecedent		Conclusion
Main	Auxiliary	
EDe	$\Delta\overline{o}_{\mathrm{f}} > \lambda_{o_{\mathrm{f}}}$ AND $\Delta\overline{e}_{\mathrm{c}} > \lambda_{e_{\mathrm{c}}}$	S_1 AND Υ_1
EDe	$\Delta\overline{o}_{\mathrm{f}} > \lambda_{o_{\mathrm{f}}}$	S_1 AND Υ_2
EDe	$\Delta d^*_{\mathrm{m}} > \lambda_{d_{\mathrm{m}}}$ AND $\Delta\overline{e}_{\mathrm{c}} > \lambda_{e_{\mathrm{c}}}$	S_2 AND Υ_1
EDe	$\Delta\overline{q}_{\mathrm{m}} < -\lambda_{q_{\mathrm{m}}}$ AND $\Delta o^*_{\mathrm{f}} < \lambda_{o^*_{\mathrm{f}}}$	S_2 AND Υ_2
EDe	$\Delta d^*_{\mathrm{m}} > \lambda_{d_{\mathrm{m}}}$	S_2 AND Υ_2
EDe	$\Delta\overline{q}_{\mathrm{m}} < -\lambda_{q_{\mathrm{m}}}$ AND $\Delta o^*_{\mathrm{f}} < \lambda_{o^*_{\mathrm{f}}}$ AND $\Delta\overline{e}_{\mathrm{c}} > \lambda_{e_{\mathrm{c}}}$	S_2 AND Υ_2
EDe	$\Delta o^*_{\mathrm{f}} < \lambda_{o^*_{\mathrm{f}}}$ AND $\Delta d^*_{\mathrm{m}} < \lambda_{d^*_{\mathrm{m}}}$	S_3 AND Υ_1
EDe	$\Delta o^*_{\mathrm{f}} < \lambda_{o^*_{\mathrm{f}}}$ AND $\Delta d^*_{\mathrm{m}} < \lambda_{d^*_{\mathrm{m}}}$ AND $\Delta\overline{e}_{\mathrm{c}} > \lambda_{e_{\mathrm{c}}}$	S_3 AND Υ_2

Fig. 9. Grinding units in the plant.

Once a type of overload condition is diagnosed, the overload adjustor will adjust the system operation according to the following expert rules to make the GML move away from the overload condition:

$$\mathrm{R}_{ij}: \begin{cases} \text{IF } S_i \text{ AND } \Upsilon_j \\ \text{THEN} \begin{cases} \Delta o^*_{\mathrm{f,L}} = \gamma_1^{(i,j)} \left[u_{e_{\mathrm{m}}}(t) - \overline{e}_{\mathrm{m}}(t)\right] \\ \Delta d^*_{\mathrm{m,L}} = \gamma_2^{(i,j)} \left[u_{e_{\mathrm{m}}}(t) - \overline{e}_{\mathrm{m}}(t)\right] \\ \Delta d^*_{\mathrm{c,L}} = \gamma_3^{(i,j)} \left[u_{e_{\mathrm{m}}}(t) - \overline{e}_{\mathrm{m}}(t)\right] \end{cases} \end{cases}$$

where $\gamma_k^{(i,j)}$, $i \in \{1,2,3\}$, $j \in \{1,2\}$, $k = 1,2,3$ stand for the adjustable coefficients, which usually are demarcated by the domain experts according to the real process characteristics.

Remark 6: The proposed methodology/algorithm can be constructed for complex industrial processes due to its hybrid strategy for different parts of the control system. The rule bases of the FDA and the ODAM can be obtained from experiential data and expert knowledge. The steady-state optimization model and the PPS soft-sensor model can be developed with the prior data, if the process has been running for some time, or with sampled data obtained by industrial experiments, if the process is new.

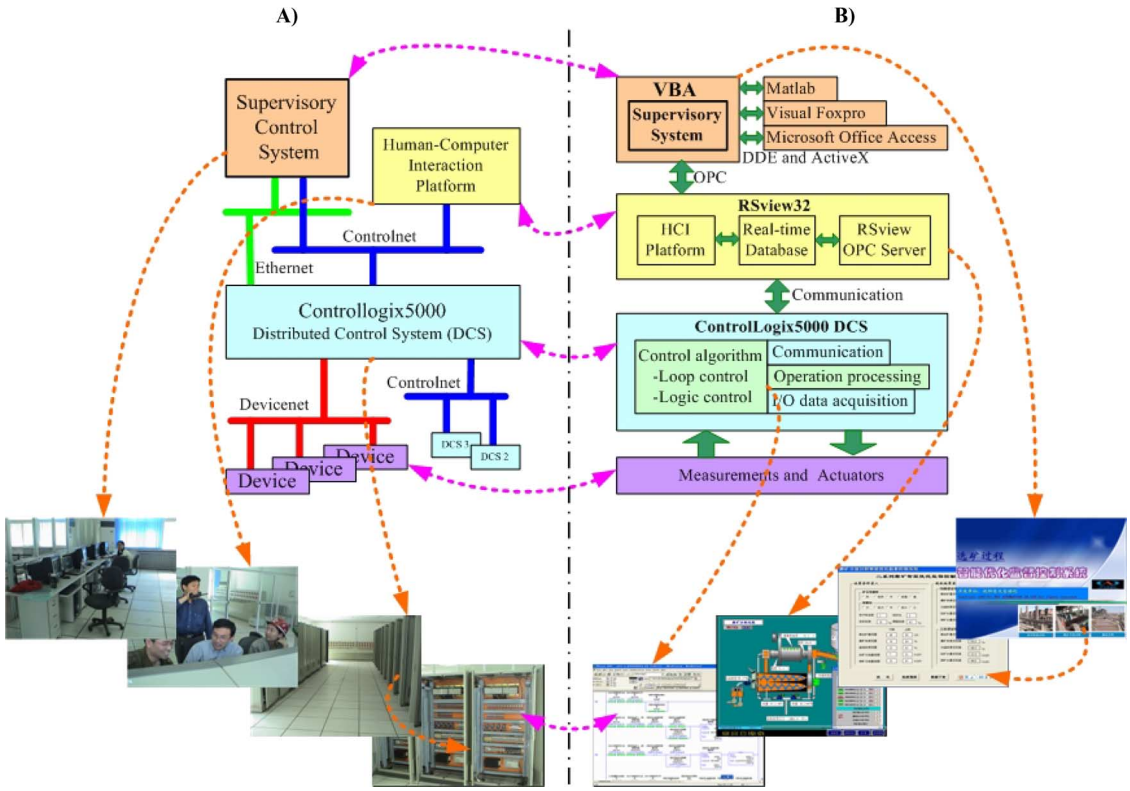

Fig. 10. Architecture of the developed grinding control system.

V. Industrial Application

Using the proposed method, an intelligence-based supervisory control system has been developed and applied to the grinding unit of a large mineral processing plant in China, as shown in Fig. 9. The general architecture of the hierarchical control system is shown in Fig. 10, whose main components and their associated key functions are described as follows.

- The Controllogix5000 DCS from Rockwell Co. was applied for lower-level loop control, logic control, sequence control, I/O data acquisition, alarm setting and network communication, etc.
- The RSView32-based human computer interface platform was developed for human operating and monitoring. Such manual supervisions include monitoring the equipment status, displaying the process parameters, querying the historical trends, listing the system alarms, operating start-stop equipments, printing the production report, and carrying out system security management and user management, etc.
- The higher-level intelligent supervisory system is completed with the visual basic application language supported by RSView32. The intelligent supervisory system can realize communication or data exchange with the DCS, human computer interface platform, and other application languages expediently, such as MATLAB, Microsoft Office Access and Visual FoxPro. MATLAB is used to perform some necessary calculation. Access and FoxPro are used to develop the data base for the supervisory system.

In order to explore the optimal operation of the grinding process, a number of industrial experiments were carried out to evaluate the control performance of the hierarchical control system. Fig. 11 shows the control effect of the PPS with the proposed supervisory control under the normal working condition. Under the initial nominal set-points $Y_0^* = [o_{\mathrm{f},0}^* d_{\mathrm{m},0}^* d_{\mathrm{c},0}^*] = [69.01\ \mathrm{t/h}, 76\%, 45.18\%]$ given by the LSOM, s_{p} and s_{a} are within the desired range $(s_{\mathrm{d}} - s_{\Delta}, s_{\mathrm{d}} + s_{\Delta})$ from the start time to $t = 150$ min. The results show the validity of the LSOM.

At $t = 150$ min, observe that $s_{\mathrm{p}} = 66\% < 200$ mesh exceeds the desirable range (60, 64)% <200 mesh, which indicates that the grinding products do not meet the specification. Thus the FDA is switched on to carry out the following calculations.

- Calculate $\Delta \mathrm{s}_{\mathrm{pd}} = 4$ and read $v_{\mathrm{m}} = 45\%$.
- Make the decision to increase o_{f}^* according to the coordination mechanism.
- Obtain $\Gamma(\Delta \mathrm{s}_{\mathrm{pd}}) = \{\mathrm{PM}\}$ and $\Gamma(v_{\mathrm{m}}) = \{\mathrm{ZO}\}$ from the membership functions and the universes.
- Obtain $\Gamma(\sigma_{\mathrm{M}_1}) = \Gamma(\sigma_{\mathrm{M}_2}) = \{\mathrm{PB}\}$ from the fuzzy rule bases.
- Employ (6) to defuzzify, we obtain $\Delta o_{\mathrm{f,M}}^* = 4.0$ t/h.
- Renew o_{f}^* as $o_{\mathrm{f}}^* = 73.41$ (t/h).

At $t = 450$ min, observe s_{p} exceeds the desirable range. Because $s_{\mathrm{p}} = 58.8\% < 200$ mesh, thus the FDA adjusts $d_{\mathrm{m}}^*, d_{\mathrm{c}}^*$, but not o_{f}^*. Due to the above fuzzy adjustments, the PPS gradually enters the desired range again. Moreover, the throughput per unit of mill has been increased. Such results show the effectiveness of the FDA.

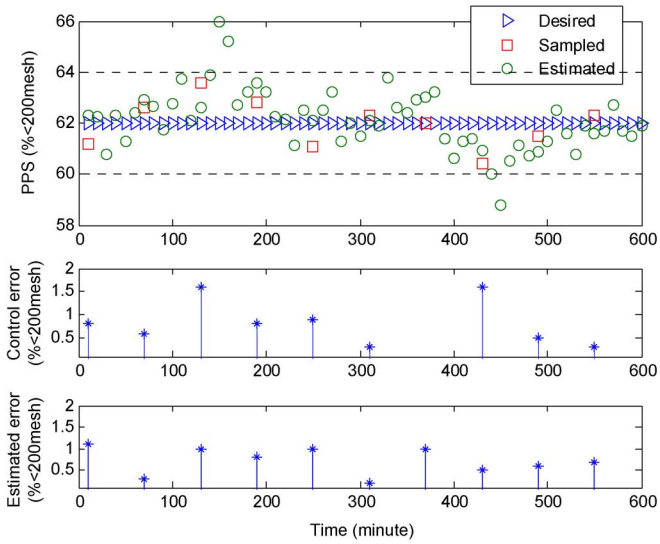

Fig. 11. Control effect of the PPS with proposed supervisory control approach under the normal working condition. The sampled PPS is provided by offline assessment. The interval of sampling is 1 hr. The estimated PPS is weighted averages of the soft-sensor outputs within 10 min. The zone between two dashed-dotted lines is the desired range.

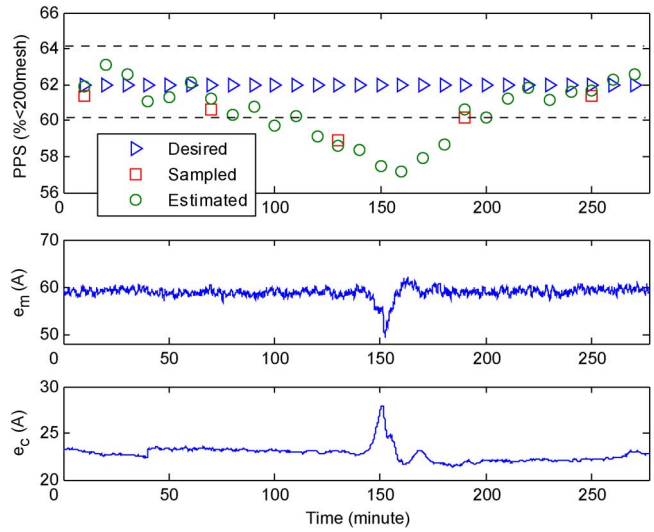

Fig. 12. Control curves of the PPS with proposed supervisory control approach under the overload working condition. The sampled PPS is provided by offline assessment with sampling interval of 1 hr and the estimated PPS is weighted averages of the soft-sensor outputs within 10 min. The zone between two dashed-dotted lines is the desired range.

Fig. 11 also shows that the estimated and controlled errors of PPS at the sampling time points are small and acceptable, which further demonstrate the good control performance of the PPS with the proposed approach and the fine estimation performance of the PSM. Fig. 12 shows the system response with the proposed supervisory control under the overload working condition. Here, the overload condition S_3 is recognized by the expert-based overload diagnosis model. Once the overload adjustor modifies the operating points, the GML moves away from the overload fault gradually. Meanwhile, the updated set-points of the grinding system make the PPS returns to the desired range. The results demonstrate the effectiveness of the expert-based ODAM algorithm.

Fig. 13 shows the comparisons of process operation performance with the human-supervised DCS scheme and the proposed intelligent supervisory control methodology under the similar working condition. As shown in Fig. 13-I-A and Fig. 13-II-A, the sampled values of PPS with supervisory control have smaller fluctuation, and are almost within the desired range. Much longer time running data also show that the statistical average of the PPS with the same desired range $60 \sim 64\% < 200$ mesh has been increased from 59.5% $<$ 200 mesh with human supervision to 62.4% $<$ 200 mesh with supervisory control, thereby confirming that the PPS has been improved with the proposed approach.

It can be observed from Fig. 13-I-B and Fig. 13-II-B that the hour averages of o_{f} with supervisory control is improved greatly compared to that with manual supervision, which means that the mill throughput is increased. This improvement is also reflected in the mill throughput and operative ratio, as can be seen from Fig. 14. According to the statistical analysis, improvements of around 5.87% and around 4.55% are achieved for the mill throughput and operative ratio, respectively, indicating that the advantage of the proposed control scheme. On the other hand, the improvement of operative ratio of the mill also illustrates that the operational breakdown caused by faulty working conditions has been decreased. This feature of proposed control system can be attributed to the ODAM.

From Fig. 13-I-C, 13-I-D, 13-II-C, and 13-II-D, one can observe that e_{m} and e_{c} are increased remarkably. It is well known that larger e_{m} and e_{c} indicate higher mill load and circulating load, respectively. Such results further illustrate that the GPR has been improved. As we know, high gain of the circulating load and the mill throughput is likely going to lead to the mill being overloaded. Therefore, the grinding system with the human supervision has to operate at a relatively conservative operating point for safety of the grinding production. However, since the ODAM can detect and adjust the mill overload by observing the variations of $e_{\mathrm{m}}, e_{\mathrm{c}}, o_{\mathrm{f}}, d_{\mathrm{m}}, q_{\mathrm{m}}$, the grinding system with intelligent supervisory control can operate at a more effective operating point with larger circulating load and mill throughput.

Fig. 15 shows the probability distribution curves of e_{m} by human-supervision and supervisory control methodology, where the dashed lines LCL are the 3-sigma (3δ) lower control limit (i.e., $u - 3\delta$) of e_{m}. From the comparison, we can conclude that the probability distribution of e_{m} with supervisory control obeys a more standardized normal distribution than that with human supervision. Their corresponding distribution parameters are $u = 60.17$, $\delta = 0.57$ for the intelligence-based system and $u = 57.55$, $\delta = 0.83$ for the human-operated system, respectively. The percentage of e_{m} larger than the 3δ lower control limit with proposed supervisory control is 99.9% (>99.7%), which indicates that it can satisfy 3δ quality control standard in process monitoring field [18], [24]. However, the percentage of $e_{\mathrm{m}} \geq u - 3\delta$ with human supervision is 99.46% (<99.7%), thus it cannot satisfy 3δ control standard. Another benefit of the intelligent supervisory control is that a much narrower fluctuation range and a much larger average value

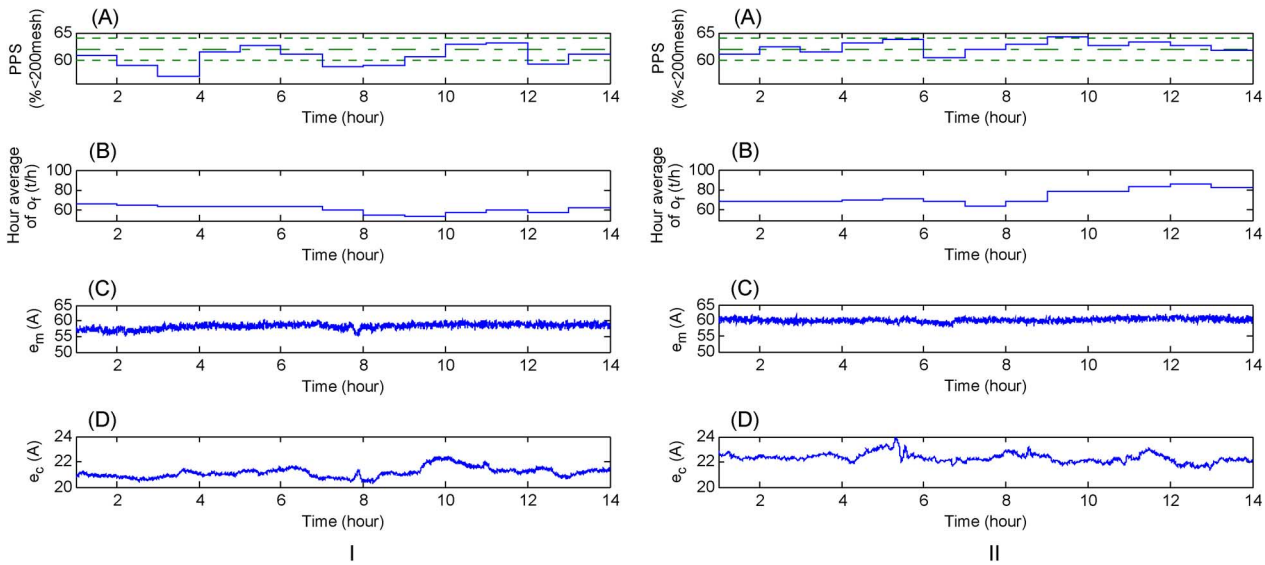

Fig. 13. Comparison of process operation performance between with human supervision (13-I) and with proposed (13-II). The sampled PPS in Fig. 13-I-A and 13-II-A are provided by assessing in laboratory with sampling interval of 1 hr.

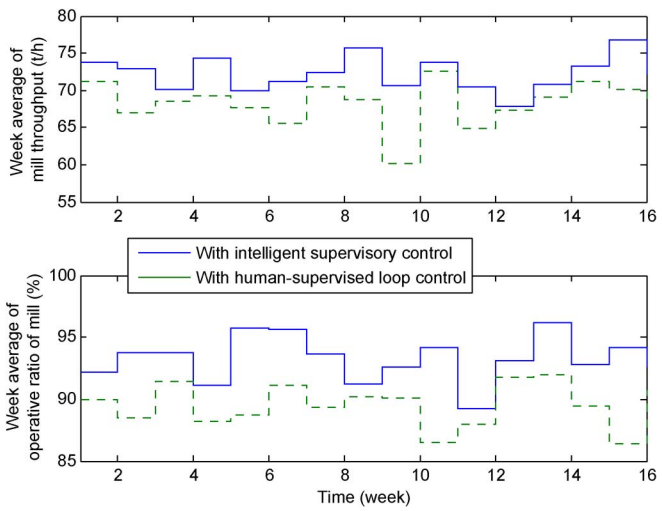

Fig. 14. Throughput per unit of mill and the operative ratio of mill with supervisory control and with human supervision. The data were taken from daily averages and then averaged into weekly figures.

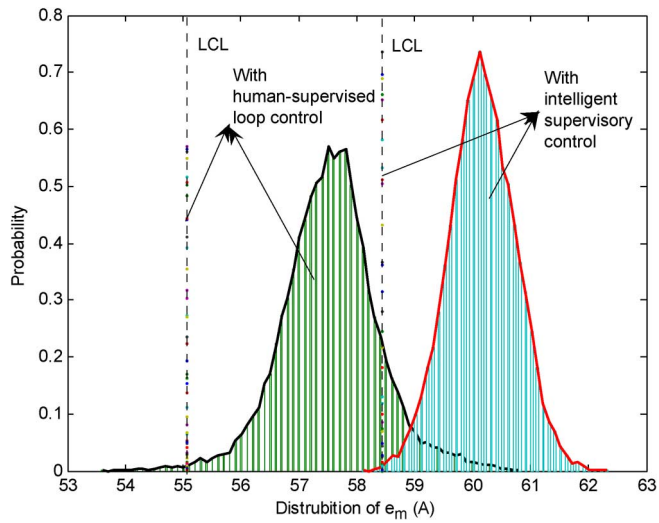

Fig. 15. Probability distribution of e_{m} with supervisory control and with human supervision.

of e_{m} have been achieved. This means the grinding system operates at the neighborhood of the optimal GML for most of the operating time. Such results show that the ODAM can monitor and control the GML well, thereby further illuminating the satisfactory overall control performance of the proposed supervisory control system.

Furthermore, the statistical data for several months indicate that the consumption of power and steel are decreased by ∼4.82% and ∼6.81%, respectively, and the equipment operation rate increases by ∼3.27%. In conclusion, the proposed supervisory control methodology has achieved an increased operation performance and notable economic benefits for the applied concentration plant.

VI. Conclusion

DCS systems have been widely used for the lower-level control in the industrial processes. Though DCS can maintain a good equipment control, determining the proper set-points under either the variation of the boundary conditions or in the presence of faulty working condition is still a difficult and crucial task to the processing industry. This paper proposed an intelligence-based supervisory control methodology that could find the proper set-points for the DCS-controlled grinding system without requiring accurate mathematical models. This approach has been applied to the grinding circuit unit of a mineral processing plant in China. As a result, the PPS has been optimized, the GPR is increased, and the energy consumption is reduced. Moreover, the overall operational efficiency of the

grinding production in terms of its reliability and stability for minimum operational breakdowns has been improved.

The work presented in this paper not only has remarkable contribution to control of the grinding process, but also shows a promising direction for controlling a wide range of processes with the following similar features.

- The production indices are difficult to be measured online directly using conventional methods or instruments, and the involved process dynamical characteristics are complicated with heavy nonlinearities and strong couplings, as well as time-varying factors or disturbances.
- The accurate models are difficult to obtain because these models vary largely in real-time with changes in boundary conditions.
- Abundant process data, operational experience, and domain-expert knowledge are available and can be used to develop the data-driven and knowledge-driven models by resorting to the intelligence-based modeling and control technique.

In this paper, we have developed and applied an ANN-based soft-sensor to estimate the grinding product particle size successfully online. There are many other process parameters, such as the GPR, the GML, and the circulating load, etc., that cannot be measured online with conventional methods. Therefore, it is also appealing to develop soft-sensors for these parameters. We believe that this is an important direction to improve the control performance for the proposed supervisory control approach, and it will be our future research topic.

ACKNOWLEDGMENT

The authors would like to thank the Associate Editor and the anonymous reviewers for their constructive comments which helped improve the quality and presentation of this paper. The authors would also like to thank Dr. Q. Liu, and Prof. C. Y. Yang for their suggestions which improved this paper.

REFERENCES

[1] C. Bouche, C. Brandt, A. Broussaud, and V. W. Drunick, "Advanced control of gold ore grinding plants in South Africa," *Mineral Eng.*, vol. 18, no. 8, pp. 866–876, 2005.

[2] M. Ramasamv, S. S. Narayanan, and C. D. P. Rao, "Control of ball mill grinding circuit using model predictive control scheme," *J. Process Control*, vol. 15, no. 3, pp. 273–283, 2005.

[3] X. S. Chen, Q. Li, and S. M. Fei, "Supervisory expert control for ball mill grinding circuits," *Expert Syst. With Appl.*, vol. 34, no. 3, pp. 1877–1885, 2008.

[4] P. Zhou and T. Y. Chai, "Intelligent monitoring and control of mill load of grinding processes," *Control Theory Appl.*, vol. 25, no. 6, pp. 1095–1098, 2008.

[5] J. Kolacz, "Measurement system of the mill charge in grinding ball mill circuits," *Minerals Eng.*, vol. 10, no. 12, pp. 1329–1338, 1997.

[6] V. R. Radharkrishnan, "Model based supervisory control of a ball mill grinding circuit," *J. Process Control*, vol. 9, no. 3, pp. 195–211, 1999.

[7] S. P. Guan, H. X. Li, and S. K. Tso, "Multivariable fuzzy supervisory control for the laminar cooling process of hot rolled slab," *IEEE Trans. Control Syst. Technol.*, vol. 9, no. 2, pp. 348–356, Mar. 2001.

[8] H. X. Li and S. P. Guan, "Hybrid intelligent control strategy. Supervising a DCS-controlled batch process," *IEEE Control Syst. Mag.*, vol. 21, no. 3, pp. 36–48, Jun. 2001.

[9] T. Y. Chai, J. L. Ding, and F. H. Wu, "Hybrid intelligent control for optimal operation of shaft furnace roasting process," *Control Eng. Pract.*, vol. 19, no. 3, pp. 264–275, 2011.

[10] T. Y. Chai, J. X. Liu, J. L. Ding, and C. Y. Su, "Hybrid intelligent control for hematite high intensity magnetic separating process," *Meas. Control*, vol. 29, no. 40, pp. 171–175, 2007.

[11] W. Wang, H. X. Li, and J. T. Zhang, "Intelligence-based hybrid control for power plant boiler," *IEEE Trans. Control Syst. Technol.*, vol. 10, no. 2, pp. 348–356, Mar. 2002.

[12] Z. J. Wang, Q. D. Wu, and T. Y. Chai, "Optimal-setting control for complicated industrial processes and its application study," *Control Eng. Pract.*, vol. 12, no. 1, pp. 65–74, 2004.

[13] E. Sebastian, "Feedback control for optimal process operation," *J. Process Control*, vol. 17, no. 3, pp. 203–219, 2007.

[14] W. Findeisen, F. Bailey, M. Brdys, K. Malinowski, P. Taijewoki, and A. Wozniak, *Control and Coordination in Hierarchical Systems*. New York: Wiley, 1980.

[15] A. C. Zanin, M. Tvrzska de Gouvea, and D. Odloak, "Industrial implementation of a real-time optimization strategy for maximizing production of LPG in a FCC unit," *Comp. Chem. Eng.*, vol. 24, no. 2–7, pp. 525–531, 2000.

[16] S. Skogestad, "Plant-wide control: The search for the self-optimizing control structure," *J. Process Control*, vol. 10, no. 5, pp. 487–507, 2000.

[17] T. Das and I. N. Kar, "Design and implementation of an adaptive fuzzy logic-based controller for wheeled mobile robots," *IEEE Trans. Control Syst. Technol.*, vol. 14, no. 3, pp. 501–510, May 2006.

[18] D. E. Seborg, T. F. Edgar, and D. A. Mellichamp, *Process Dynamics and Control*, 2nd ed. New York: Wiley, 2004.

[19] W. A. Shewhart, *Economic Control of Quality of Manufactured Product*. New York: Van Nostrand, 1931.

[20] Y. Du, R. del Villar, and J. Thibault, "Neural-net based soft-sensor for dynamic particle size estimation in grinding circuits," *Int. J. Mineral Process.*, vol. 52, no. 2–3, pp. 121–135, 1997.

[21] A. Casali, G. Gonzalez, F. Torres, G. Vallebuona, L. Castelli, and P. Gimenez, "Particle size distribution sort-sensor for a grinding circuit," *Powder Technol.*, vol. 99, no. 1, pp. 15–21, 1998.

[22] R. G. Del Villar, J. Thibault, and R. Del Villar, "Development of a soft-sensor for particle size monitoring," *Mineral Eng.*, vol. 9, no. 1, pp. 55–72, 1996.

[23] K. J. Astrom and B. Wittenmark, *Adaptive Control*. New York: Addison Wesley, 1995.

[24] D. C. Montgomery and G. C. Runger, *Applied Statistics and Probability for Engineers*, 3rd ed. New York: Wiley, 2003.

Ping Zhou received the B.S. and the M.S. degree in control theory and engineering from Northeastern University, Shenyang, China, in 2003 and 2006, respectively, where he is currently pursuing the Ph.D. degree in control theory and control science.

His research interests include the development of feedback control technologies for optimal process operation, multivariable decoupling control, and soft-sensor technologies with application to industrial process.

Mr. Zhou was the recipient of the Rockwell Automation Award for the Outstanding Application Paper at the Six World Congress on Intelligent Control and Automation.

Tianyou Chai (M'90–SM'97–F'08) received the Ph.D. degree in control theory and engineering from Northeastern University, Shenyang, China, in 1985.

He has been with the Research Center of Automation, Northeastern University, since 1985, where he became a Professor in 1988 and a Chair Professor in 2004. He is the founder and Director of the Center of Automation, which became a National Engineering and Technology Research Center in 1997. He has published two monographs, 99 peer reviewed international journal papers, and around 224 international conference papers. He has been invited to deliver over 20 plenary speeches in international conferences of IFAC and IEEE. His current research interests include adaptive control, intelligent decoupling control, integrated plant control and system, and the development of control technologies with applications to various industrial processes.

Prof. Chai is a member of Chinese Academy of Engineering, an academician of International Eurasian Academy of Sciences, and an IFAC Fellow. He is a distinguished visiting fellow of The Royal Academy of Engineering (U.K.) and an invitation fellow of Japan Society for the Promotion of Science (JSPS). For his contributions, he was a recipient of three prestigious awards of National Sci-

ence and Technology Progress, the 2002 Technological Science Progress Award from Ho Leung Ho Lee Foundation, the 2007 Industry Award for Excellence in Transitional Control Research from IEEE Control Systems Society, and the 2010 Yang Jia-Chi Science and Technology Award from Chinese Association of Automation.

Jing Sun (M'89–SM'00–F'04) received the B.S. and M.S. degrees from the University of Science and Technology of China, Hefei, China, in 1982 and 1984, respectively, and the Ph.D. degree from the University of Southern California, Los Angeles, in 1989.

From 1989 to 1993, she was an Assistant Professor with the Department of Electrical and Computer Engineering, Wayne State University. She joined the Ford Research Laboratory in 1993, where she worked in the Powertrain Control Systems Department. After spending almost ten years in industry, she returned to academia and joined the faculty of the College of Engineering, University of Michigan, Ann Arbor, in 2003, where she is now a Professor with the Department of Naval Architecture and Marine Engineering and the Department of Electrical Engineering and Computer Science. Her research interests include system and control theory and its applications to marine and automotive propulsion systems. She holds over 30 U.S. patents and has coauthored a textbook on robust adaptive control.

Dr. Sun was a recipient of the 2003 IEEE Control System Technology Award.